

Facile synthesis of highly stable α -Si by ion implantation of low-keV H isotopes

O. Moutanabbir,* R. Scholz, and U. Gösele

Max Plank Institute of Microstructure Physics, Weinberg 2, D 06120 Halle, Germany

B. Terreault

INRS-EMT, Université du Québec, 1650 Boulevard Lionel-Boulet, Varennes, Québec, Canada J3X 1S2

(Received 28 May 2009; published 23 June 2009)

It is experimentally shown that silicon is “easily” amorphized by low-keV H ions at the relatively high temperature of 150 K and for an ion fluence equivalent to <1 DPA (displacement per atom). The α -Si layer is much more stable against recrystallization than α -Si produced by other ions and more stable against chemical modification than c -Si that is H-implanted at room temperature. These results are unexplained by the current atomic collision theory, including molecular-dynamics simulations, but they demonstrate the stabilizing effect of dangling bond passivation by H atoms in postulated, metastable, amorphous droplets.

DOI: [10.1103/PhysRevB.79.233202](https://doi.org/10.1103/PhysRevB.79.233202)

PACS number(s): 61.80.Jh, 61.72.-y, 61.80.Az, 85.40.Ry

Silicon amorphization by charged particle beams is an experimentally well-established phenomenon.¹⁻³ The conditions required for its occurrence, i.e., minimum particle fluence Φ_A , beam energy, and sample temperature during irradiation, vary greatly with particle mass. Heavier ions amorphize Si at and above room temperature (RT) for low Φ_A values of the order of 10^{14} ion cm^{-2} .⁴ Amorphization at temperatures up to RT is also observed with ions as light as B⁺ but, for these, Φ_A increases rapidly with temperature above ~ 100 K.⁴ Amorphization by Li (Ref. 4) and He (Ref. 5) ions has only been seen at LN₂ temperature. Finally amorphization by electrons requires beam energies >1 MeV, temperatures ≤ 100 K, and temperature-dependent Φ_A values $\geq 10^{22}$ cm^{-2} .³ Two obvious factors explain the gross trends of these results: the magnitude of the Coulomb (or screened Coulomb⁶) collision cross section and the maximum energy transfer to primary recoils, T_{MAX} . They can be factored out, allowing the study of more subtle effects, by using concepts based on atomic collision theory, i.e., the density of energy deposited into recoils, E_{REC} (excluding electronic losses), energy deposition per atom, $E_A = E_{\text{REC}}/N$ (N =atomic density), displacement energy, E_D , and atomic displacements per atom (DPA).⁷ In binary collision descriptions of the collision cascade, e.g., the Kinchin-Pease (KP) model,⁸ the DPA $\sim E_A/2E_D$, provided that the condition $T \geq 2E_D$ apply to most primary collisions.⁷ For Si, $E_D \sim 15$ eV.⁹ On this basis, the different results have been discussed in terms of models such as collision cascade overlap,^{1,2,4} critical energy deposition,^{4,10,11} or critical defect density,^{5,12,13} thermal spikes,¹⁴ and direct amorphous pocket formation by single ions.^{1,10,15-19} Another point of considerable interest is that as-implanted α -Si is actually metastable and transforms at 300 °C–400 °C into a more stable form which, in turn, recrystallizes epitaxially at 500 °C–600 °C.^{5,20}

Conspicuously absent in the literature is the investigation of Si amorphization by H ion beams, in spite of the crucial information it could provide concerning the mass dependence and the role of Si-H chemistry. Moreover, H-induced amorphization would create new opportunities as well as new constraints in microfabrication processes such as ion slicing and thin-layer transfer.^{21,22} Yet, there are only imprecise and contradictory data.^{23,24}

This overlook is perhaps an effect of the widely prevalent belief that H-ion-induced α -Si formation would be practically impossible or at least “not easy.” Indeed, model-based data extrapolations^{4,10,13} imply it would require cryogenic temperatures and $E_A \gg E_D$ or, equivalently, a DPA $\gg 1$. Here we report transmission electron microscopy (TEM) results which show, on the contrary, that Si is “easily” amorphized by low-keV H-ion beams, that is, for a low DPA ~ 1 and a relatively high temperature of 150 K. Moreover, the as-implanted α -Si formed is highly stable. A Raman study of the Si-H bonding configuration during annealing shows that it hardly evolves [contrary to what is observed in c -Si (Refs. 25 and 26)], and the TEM results indicate that our α -Si recrystallization rate is 2 orders of magnitude smaller than that of the He-implanted α -Si.⁵

In the present work, 5 keV H or D ions were used. The samples were maintained at 150 K during implantation. They consisted of Cz-grown, 1–10 Ω cm resistivity, n -type (001) Si-wafer pieces. The ion fluences were 6×10^{16} cm^{-2} , resulting in H (D) profiles with peak atom concentrations of $\sim 15\%$ (11%), full width at half maximum of ~ 63 (87) nm, and mean range of ~ 75 (95) nm, as computed by SRIM (Ref. 9) and verified by elastic recoil detection;²⁷ computed H and D depth profiles are shown in Figs. 1(a) and 1(c). After standard cross-section preparation including thinning by ion milling, pieces of the samples were observed by transverse section electron microscopy (XTEM) at medium magnification and at high-resolution (HRXTEM), using Philips CM 20T and JEOL 4010 microscopes operated at 200 and 400 kV, respectively. On other pieces, the spectra of the local modes of Si-H/D stretch vibrations (1900–2250 cm^{-1} and 1350–1675 cm^{-1} , respectively) were acquired using a 514.5 nm Ar-ion laser in a LabRam HR800 Raman spectrometer (from Horiba Jobin Yvon). The same pieces were then annealed at high temperature to investigate the stability of the defects and of the eventual amorphous regions.

Under the above conditions, considerable amorphization does take place. With H ions, as seen in Fig. 1(a), a lighter band, 50 ± 4 nm thick and due to α -Si, appears under the thin surface layer (22 ± 5 nm). Close examination reveals scattered tiny dark spots in the α -Si layer, interpreted as Si nanocrystals; their volume fraction is negligible. HRXTEM

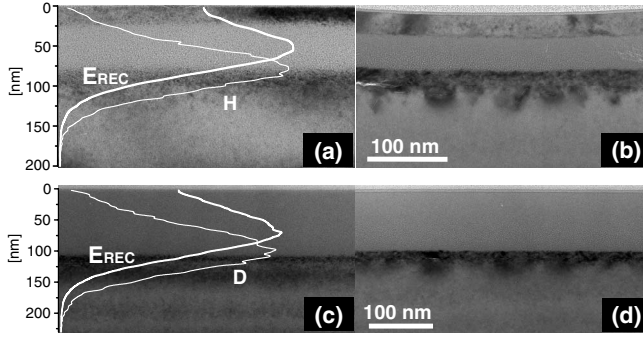


FIG. 1. (a) XTEM images of silicon implanted with H ions at 150 K, as-implanted and (b) after annealing at 825 K for 300 s; (c) and (d) are the corresponding images for D-implanted Si. In (a) and (c) the depth profiles of the ions and of the energy deposition into recoils (E_{REC}) calculated by the code SRIM are superposed (arbitrary intensity scales).

[Fig. 2(a)] shows that the first interface ($c\text{-Si}/a\text{-Si}$) is rough and contains relatively large inclusions of $c\text{-Si}$ in $a\text{-Si}$ and vice versa. The second interface ($a\text{-Si}/c\text{-Si}$) rests, perhaps fortuitously, at about the peak in the H concentration (75 nm). With D ions [Fig. 1(c)] the amorphous zone starts right at the surface and extends down to 101 ± 2 nm. Again, the second interface happens to nearly coincide with the peak in D concentration (95 nm). The layer thickness measurements are summarized in Table I. Beyond the $a\text{-Si}$ layer, a zone of heavy damage is apparent.

Let us first consider these results in terms of the critical energy density model,^{4,10,11} i.e., critical E_{REC} . The local values of E_A can be calculated using the E_{REC} values given by

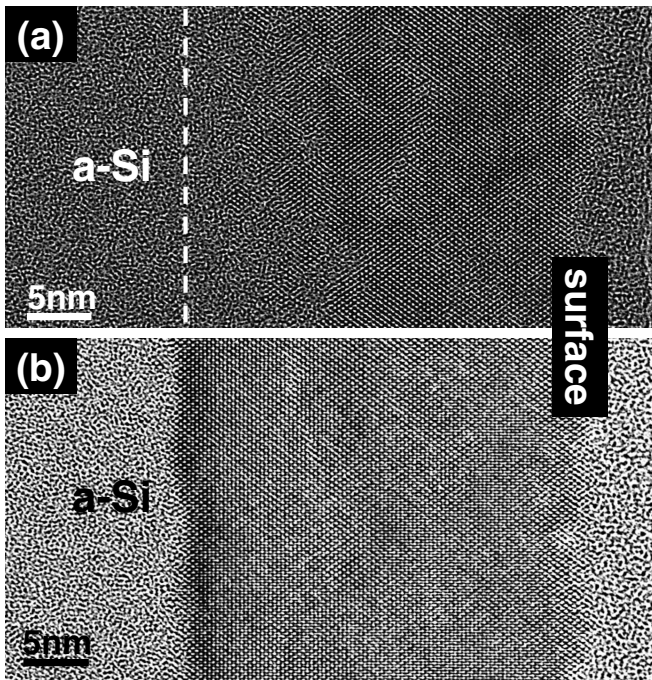


FIG. 2. (a) HRXTEM images in the vicinity of the surface for Si implanted with H ions at 150 K, as-implanted and (b) after annealing at 825 K. The dashed line marks the postannealing $a\text{-Si}/c\text{-Si}$ interface.

TABLE I. Thicknesses of the $c\text{-Si}$ and $a\text{-Si}$ layers for H- and D-implanted Si, as-implanted or after annealing at 825 K for 300 s.

Layer	Layer thickness (nm)			
	H as-implanted	H annealed	D as-implanted	D annealed
$c\text{-Si}$	22 ± 5	28 ± 4	0	4–5
$a\text{-Si}$	50 ± 5	42 ± 4	101 ± 2	95 ± 2

SRIM,⁹ [see also Figs. 1(a) and 1(c)]. If we apply this scheme to our data, we obtain the following values with H ions: at the first interface ($c\text{-Si}/a\text{-Si}$), $E_A(\text{H})=18$ eV/atom, and at the second one ($a\text{-Si}/c\text{-Si}$), $E_A(\text{H})=19$ eV/atom, values close to the conventional $E_D=15$ eV, and comparable to the 12 eV/atom (Ref. 4) to 20 eV/atom (Ref. 10) obtained at 80 K or with heavy ions. It implies that little dynamic annealing took place during the implantation at 150 K. In the case of D ions, at the surface, SRIM gives $E_A(\text{D})=30$ eV/atom, considerably above the threshold found for H, thus explaining why the amorphous layer reaches the surface. However, at the second interface, $E_A(\text{D})=41$ eV/atom is found, yet the material *reverts* to the crystalline form. These findings demonstrate the very approximate character of the simple approach in the present case.

To estimate the critical defect density for amorphization, one cannot use the simple KP formula because the typical energy of primary recoils does not satisfy $T \gg E_D$; this can be seen in Table II, where the contributions to E_{REC} of recoils in different energy ranges are displayed. Instead we use SRIM in the full cascade simulation mode with $E_D=15$ eV. For H, SRIM gives 6.8 displacement/ion within the $\sim 110\text{-nm}$ -thick implanted layer [Fig. 1(a)], equivalent to 0.7 DPA, and for D, 19.4 displacement/ion within ~ 140 nm or 1.6 DPA. These

TABLE II. The maximum T values and the relative contributions of different energy ranges (ΔT) to total E_{REC} are compared for 5 keV H and D ions, 120–200 keV He ions and 2 MeV electrons. The characteristic recoil energies of 2, 15, and 100 eV correspond to the atomic binding energy, the displacement energy, and the minimum energy to generate hot cascades, respectively. The displayed number is the integral of $T(d\sigma/dT)dT$ over the interval ΔT , normalized to the total E_{REC} . For H and D ions, the Lindhard-Scharff-Schiott theory (Ref. 6) was applied using an effective ion energy along the ion path of 3 keV; for 120–200 keV He, Coulomb scattering was applied assuming an ion energy of 20 keV near the end of range where damage production peaks; for 2 MeV electrons, relativistic Coulomb scattering was applied (Ref. 7, p. 124).

	5 keV H	5 keV D	120–200 keV He ^a	2 MeV electron
T_{MAX} (eV)	400	747	8740	459
ΔT (eV)	Fraction of total E_{REC}			
2–15	0.27	0.20	0.24	0.43
15–100	0.50	0.38	0.23	0.39
>100	0.23	0.42	0.53	0.18

^aIn the work of Ref. 5, the samples were successively implanted at 120 and 200 keV.

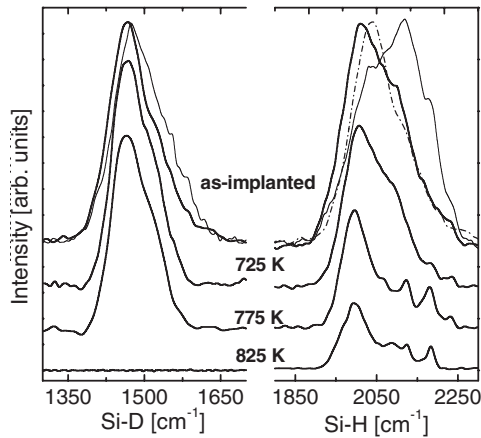


FIG. 3. Thermal evolution of Raman spectra of Si-H/D local vibrational (stretch) modes. The spectra for H/D implantation at 150 K (thick lines) and at RT (thin lines) are compared. The dashed-dotted line presents the rescaled Si-D spectrum obtained at 150 K.

are comparable to the value for He at 77 K, namely, 1 DPA.⁵ Thus, H-induced amorphization is somewhat “easier” than the He-induced amorphization, in spite of the higher temperature and the fact that both the maximum and the average recoil energies are smaller for H or D ions than for He ions, see Table II. We also note in the table that 5 keV H ions and 2 MeV electrons give comparable maximum T and not too different T distributions, yet the requirements for amorphization are extremely different. Indeed, for 2 MeV electrons, the critical DPA amounts to 5 DPA at 25 K, and it increases rapidly with temperature to 13 DPA at 80 K and 35 DPA at 100 K; and for 1 MeV electrons, it reaches 130 DPA, always at 25 K.³ Clearly, binary collision theory is insufficient to account for the observed amorphization thresholds for light-charged particles.

In the case of heavy-ion amorphization, characterized by low critical DPA of order 1 even above LN₂ temperature, amorphous pockets with sizes of several nanometers have been observed^{1,15,16} to be generated directly within single-collision cascades. That process is understood to result from the quenching of large and dense cascades in which the “temperature” (average atom kinetic energy) is substantially higher than the melting point of silicon. In the binary-collision approximation, this mechanism requires primary recoils of at least 1 keV,¹³ so it cannot apply to our case, see Table II. But some recent molecular-dynamics simulations have suggested that the “1 keV criterion” can be relaxed. Beck *et al.*¹⁷ showed that 100 eV recoils generated $\sim 1\text{-nm}^3$ -sized cascades in which a majority of atoms were displaced and/or had a temperature >0.2 eV, i.e., above the Si melting point. However, Hobler and Otto¹⁸ and Santos *et al.*¹⁹ found that actual melting required a cascade temperature ≥ 2 eV, an order of magnitude higher than Beck’s 0.2 eV. So, although a non-negligible fraction of E_{REC} for 5 keV H and D ions is due to recoils with $T > 100$ eV, i.e., 23% and 42%, respectively (Table II), according to the current theory the conditions for direct a -Si pocket formation would not be met in the present case. Besides, if they were for keV H ions, they would also be met for MeV electrons which give rise to similar recoil distributions (Table II), in striking

contradiction with the data of Takeda and Yamasaki.³ However, the cited models do not take into account the chemical reactivity of the implanted species.

The chemical role of hydrogen is investigated next. In Fig. 3 are displayed the Raman spectra in the region of the Si-H/D local stretch modes for the H/D-implanted amorphized samples and, for comparison, for still crystalline samples implanted at RT with the same ion fluence (thin lines). For the latter, the Si-H spectrum peaks at high wave number around 2115 cm^{-1} ; this mode has been shown to be due to the Si-H₂ stretch vibration for hydrogen dimers adsorbed on internal Si(001) surfaces.^{25,26} Shoulders are also present at 2030 cm^{-1} (H or H₂ in divacancies, V₂H_{1,2}), 2180 cm^{-1} (V₂H₆), and 2235 cm^{-1} (VH₄). In contrast, in the amorphized sample, the spectrum peaks at low wave number around 2010 cm^{-1} ; this wave number is slightly below that for V₂H_{1,2} and above the single Si-H mode reported for hydrogenated a -Si ($\sim 2000\text{ cm}^{-1}$).²⁸ Just as vacancies and small clusters are stabilized in c -Si, similarly H attachment to dangling bonds stabilizes a -Si. Note that the Si-H band appears to be broader than in the case of H-implanted a -Si.²⁹ This comes from the overlap of different modes originating from c -Si and a -Si regions. Unlike Si-H, the Si-D Raman modes seem to vary less with implantation temperature. The dominant mode at 150 K is observed around 1467 cm^{-1} . To compare with Si-H modes, the frequency of the Si-D spectrum was rescaled by a factor of 1.39 (dashed line in Fig. 3). The rescaled Si-D spectrum is shifted up by $\sim 30\text{ cm}^{-1}$ compared to Si-H suggestive of H and D trapping in different structures. The Si-D band most likely originates from both single (Si-D) and double (Si-D₂) bond modes.²⁸ It is also worth pointing out that H₂/D₂ molecule formation and agglomeration in multivacancies, as observed in RT implantation,³⁰ do not take place at 150 K, indicating a more effective trapping of H/D.

We study next the high-temperature stability of the amorphous layers. Figures 1(b) and 1(d) display micrographs of the H- and D-implanted samples after annealing at 825 K for 300 s. At both ends, in the H-implanted sample, recrystallization has taken place (Table I), and the process is epitaxial as shown in the high-resolution picture in Fig. 2(b). Nanovoids have appeared in the deeper part of the a -Si layers [Figs. 1(b) and 1(d)]. The heavy damage layers now show platelets and cracks, which have evolved into large blisters in the case of H but not D. The occurrence of blistering implies that the very thin ($<100\text{ nm}$) and high-quality c -Si/ a -Si/ c -Si multilayer structure created here could be splitted off and transferred onto another wafer by the usual “ion-cutting” process;²¹ this could have interesting applications, e.g., by taking advantage of the differences in the electronic and optical properties of the different layers.

The thermal evolution of the Si-H/D Raman spectra in Fig. 3 is revealing. For H, at 775 and 825 K, the low wave-number peak due to H chemisorbed in a -Si has decreased considerably, possibly by evaporation of H₂. The high wave-number peaks due to Si-H₂ on internal surfaces and V₂H₆ have emerged, albeit much more weakly than in RT-implanted Si;²⁶ those last modes are undoubtedly connected with the c -Si beyond the a -Si layer since the lines are narrow. For D, the low wave-number peak remains surprisingly

stable up to 775 K but disappears suddenly at 825 K. There are thus some differences between the behaviors of the two isotopes; there must be subtle differences in the atomic-level structure of the *a*-Si layers produced by the two isotopes, likely related to the higher energy of the D-generated recoils. However, one fact is clear: abundant H and D remain bound in essentially the same state in *a*-Si up to at least 775 K whereas in *c*-Si, H and D undergo a whole series of transformations starting from ~ 550 K.^{25,26} It thus appears that the Si-H/D bonds in *a*-Si result in an increase in the thermodynamic barrier against transformation. Indeed, the recrystallization rate in the H-implanted sample was found to have an upper limit of ~ 0.025 nm/s, much lower than that of *a*-Si created by He implantation, which, at the same temperature of 825 K, amounts to ~ 1 nm/s for as-implanted Si, and ~ 0.1 nm/s for relaxed (annealed) *a*-Si.⁵ Moreover, in the D-implanted sample, the recrystallization rate is even smaller.

To conclude, we have demonstrated that low-keV H- or D-ion bombardment amorphizes silicon rather easily at 150 K. A comparison with the cases of He and electron irradiation leads to the conclusion that the requirements for H-ion induced cannot be extrapolated from other data on the basis

of current theory, including sophisticated molecular-dynamics computations of collision cascades¹⁷ and melting of hot disordered pockets.^{18,19} Only tiny (\sim nm) and insufficiently hot (0.2 eV) disordered pockets can possibly be generated by H- or D-induced cascades. However, by attaching readily to dangling bonds, H atoms raise considerably the thermodynamic barrier required to revert to *c*-Si. We conjecture that, in this way, incipient and metastable *a*-Si drops are stabilized and can thus accumulate during the bombardment until a continuous *a*-Si layer is formed. Moreover, as a consequence, the amorphous layer is much more stable under high-temperature annealing than layers formed by implantation of more inert ions. Electronic and/or photonic applications of these results can be envisaged.

Heartfelt thanks are extended to A. Giguère (INRS-EMT) for the implantations, M. Chicoine (Université de Montréal) for the elastic recoil detection measurements, and S. Hopfe (MPI-Halle) for TEM preparation. This work was supported by NSERC (Canada), FQRNT (Québec), and the German Federal Ministry of Education and Research (Contract No. 01BU0624, CrysGaN).

*moutanab@mpi-halle.mpg.de

- ¹D. J. Mazey, R. S. Nelson, and R. S. Barnes, *Philos. Mag.* **17**, 1145 (1968).
- ²F. F. Morehead and B. L. Crowder, *Radiat. Eff.* **6**, 27 (1970).
- ³S. Takeda and J. Yamasaki, *Phys. Rev. Lett.* **83**, 320 (1999).
- ⁴J. R. Dennis and E. B. Hale, *J. Appl. Phys.* **49**, 1119 (1978).
- ⁵S. Roorda, W. C. Sinke, J. M. Poate, D. C. Jacobson, S. Dierker, B. S. Dennis, D. J. Eaglesham, F. Spaepen, and P. Fuoss, *Phys. Rev. B* **44**, 3702 (1991).
- ⁶J. Lindhard, M. Scharff, and H. E. Schiøtt, *Mat. Fys. Medd. K. Dan. Vidensk. Selsk.* **33**, 1 (1963).
- ⁷M. W. Thompson, *Defects and Radiation Damage in Metals* (Cambridge University Press, Cambridge, England, 1969).
- ⁸G. H. Kinchin and R. S. Pease, *Rep. Prog. Phys.* **18**, 1 (1955).
- ⁹J. F. Ziegler and J. P. Biersack, the stopping and range of ions in matter, www.srim.org
- ¹⁰J. F. Gibbons, *Proc. IEEE* **60**, 1062 (1972).
- ¹¹F. L. Vook, in *Radiation Damage and Defects in Semiconductors*, edited by J. E. Whitehouse (Institute of Physics, London, 1972), p. 60.
- ¹²L. A. Christel, J. F. Gibbons, and T. W. Sigmon, *J. Appl. Phys.* **52**, 7143 (1981).
- ¹³G. Hobler and G. Otto, *Mater. Sci. Semicond. Process.* **6**, 1 (2003).
- ¹⁴D. A. Thompson, *Radiat. Eff.* **56**, 105 (1981).
- ¹⁵L. M. Howe *et al.*, *Nucl. Instrum. Methods* **170**, 419 (1980).
- ¹⁶J. Narayan *et al.*, *Mater. Lett.* **3**, 67 (1985).
- ¹⁷M. J. Beck, R. D. Schrimpf, D. M. Fleetwood, and S. T. Pantelides, *Phys. Rev. Lett.* **100**, 185502 (2008).
- ¹⁸G. Hobler and G. Otto, *Nucl. Instrum. Methods Phys. Res. B* **206**, 81 (2003).
- ¹⁹I. Santos, L. A. Marques, and L. Pelaz, *Phys. Rev. B* **74**, 174115 (2006).
- ²⁰J. S. Lannin, *J. Non-Cryst. Solids* **97-98**, 39 (1987).
- ²¹M. Bruel, *Electron. Lett.* **31**, 1201 (1995).
- ²²B. Terreault, *Phys. Status Solidi A* **204**, 2129 (2007).
- ²³J. K. G. Panitz, D. J. Sharp, and C. R. Hills, *J. Vac. Sci. Technol. A* **3**, 1 (1985).
- ²⁴T. Hara *et al.*, *Jpn. J. Appl. Phys.* **39**, 4427 (2000).
- ²⁵M. K. Weldon *et al.*, *J. Vac. Sci. Technol. B* **15**, 1065 (1997).
- ²⁶O. Moutanabbir and B. Terreault, *J. Chem. Phys.* **121**, 7973 (2004).
- ²⁷Measurements carried out by M. Chicoine at the Tandem Accelerator Laboratory, Université de Montréal.
- ²⁸M. H. Brodsky, M. Cardona, and J. J. Cuomo, *Phys. Rev. B* **16**, 3556 (1977).
- ²⁹H. J. Stein, *Phys. Rev. Lett.* **43**, 1030 (1979).
- ³⁰O. Moutanabbir, B. Terreault, M. Chicoine, F. Schiettekatte, and P. J. Simpson, *Phys. Rev. B* **75**, 075201 (2007).